PROCEEDINGS OF SCIENCE

On systematic uncertainties of the AugerPrime Radio Detector

Tomáš Fodran[a,*] **for the Pierre Auger Collaboration**[b,†]

[a] *Department of Astrophysics/IMAPP, Radboud University, P.O. Box 9010, NL-6500 GL Nijmegen, The Netherlands*

[b] *Observatorio Pierre Auger, Av. San Martín Norte 304, 5613 Malargüe, Argentina.*

E-mail: f.author@inst.edu, s.author@univ.country

A major upgrade of the Pierre Auger Observatory, AugerPrime, whose main purpose is to improve mass sensitivity studies, will soon be completed. The role of the AugerPrime Radio Detector is to extend the mass-sensitive measurements to high zenith angles above 65 degrees. The power to discriminate between different cosmic ray species in the reconstruction depends on the systematic and statistical uncertainties of the reconstruction algorithm. The main cause of systematic uncertainties of the Radio Detector is the difference between the antenna model and the actual practical implementation. To determine this uncertainty, we reconstruct CORSIKA/CoREAS Monte Carlo air shower simulations using an antenna model geometry, slightly modified in various ways. In addition, we also study the influence of different ground conditions. This work aims to determine a realistic systematic uncertainty of the electromagnetic energy reconstructed from the Radio Detector.

9th International Workshop on Acoustic and Radio EeV Neutrino Detection Activities - ARENA2022
7-10 June 2022
Santiago de Compostela, Spain

*Speaker

†Full author list at https://www.auger.org/archive/authors_2022_06.html.

PoS(ARENA2022)043

1. Introduction

The much-expected AugerPrime upgrade of the Pierre Auger Observatory will soon be completed [1]. After the upgrade, the Surface Detector stations will comprise of a Radio Detector (RD), a surface scintillator detector (SSD), and an additional small photo-multiplier tube for the water-Cherenkov detector (WCD). The main goal of this upgrade is a precise measurement of the mass composition of cosmic rays. The role of the RD is to provide electromagnetic energy measurements above 65° zenith angles providing a tool that, in tandem with the WCD, will allow studying mass composition at these high zenith angles. Currently, ten out of the planned 1661 stations have been upgraded with RD antennas, forming an engineering array. We expect to complete the RD upgrade in 2023. For more technical information about the RD antenna, see [2, 3].

It is obvious to expect small differences between the (ideal) antenna model and the actual (practical) setup. For example, the antenna can be a little tilted or rotated, or other components of the WCD, such as the SSD or solar panel, can be slightly shifted. Moreover, the whole station could be tilted due to soil settlement. These types of deviations we refer to as geometrical uncertainties. They may randomly vary from station to station. Another important factor that can cause a deviation is the physical performance of the ground. In the Pierre Auger Observatory's 3000 km^2 array, the ground conditions change from place to place and also with the weather and seasons. For instance, the conductivity of dry and wet sandy soil changes from $10^{-4} - 10^{-2}$ to $10^{-2} - 10^{-1}$ [S/m], respectively and relative permittivity from $4 - 6$ to $15 - 30$ [F/m].

In this contribution, we aim to determine the RD systematic uncertainty caused by deviations (systematic uncertainties) between the antenna model and the actual construction, which affects the event-to-event reconstruction and the absolute calibration. In the first part, we objectively quantify the propagated effect of this uncertainties on the reconstructed electromagnetic energy. In the second part, we evaluate the uncertainty caused by the geometrical uncertainties on the absolute calibration. Ultimately, we report about our efforts on the absolute galactic calibration on a day-to-day basis.

2. Event-to-event reconstruction and related uncertainties

2.1 Method

When reconstructing simulated data, the hardware response (including the antenna model) has to be applied twice - first on the so-called "forward" and then on the so-called "backward" response. On the forward response, we get the simulated response at our hardware, in particular the ADC traces in the digitizer. This stage simulates measured data. The process then continues as with the measured data, the backward response is applied, the stations' electric fields and energy fluencies are reconstructed, and the electromagnetic energy is derived from the lateral distribution function fit.

Using the same antenna model for forward and backward responses represents our "ideal scenario" where all antennas in the field are assumed to be identical and fully agree with the idealized antenna model used on the backward response. In our "realistic scenario", we randomly change station parameters within their expected systematic uncertainties and assign modified models to stations on the forward response. For the backward response, we use the idealized model for

Table 1: Antenna models with modified geometrical parameters to study the effects of systematic geometrical uncertainties.

modification	direction of the modification	magnitude	total # of models
tilted antenna	cardinal and intercardinal	1°, 2°, 3°, 4°, 5°	40
rotated antenna	clockwise, counterclockwise	1°, 2°, 3°, 4°, 5°	10
tilted station	cardinal and intercardinal	1°, 2°, 3°	24
shifted SSD	cardinal and vertical	20 cm (E,W,N), 0.8 cm (S), 10 cm "up"	5
solar panel	cardinal and vertical ("up")	20 cm	5

Table 2: Permittivities and conductivities of the ground used to study the resulting systematic uncertainties.

	permittivity	conductivity [S/m]	description
default	5.5	0.0014	AERA standard ground condition[5]
ground 1	3	0.0004	Extremly poor ground
ground 2	5	0.001	Very poor ground
ground 3	10	0.002	Poor ground 1
ground 4	13	0.002	Poor ground 2
ground 5	13	0.005	Average ground
ground 6	20	0.0303	Very good ground
ground 7	81	5	Excellent ground

all stations. We used the modified models listed in Tab. 1 to the study effects of geometrical uncertainties. For the influence of different ground conditions, we use seven different sets of parameters as listed in Tab. 2. In total, we used 91 antenna models for this study. The antenna model simulations were performed in 4NEC2 software [4]. The modified models are used to mimic simplified cases of possible systematic variations in the station set-up. In reality, one might expect various combinations of these variations and others, e.g., deformation of the circular antenna loop.

We reconstructed 2000 proton Corsika/Coreas simulations for realistically spaced energies, azimuth, and zenith angles for ideal and realistic scenarios and compare the reconstructed electromagnetic energies on event-to-event basis. For each studied systematic deviation, we repeated this procedure for five different random seeds.

For geometrical uncertainties (tilt and rotation), we assume either linearly decaying or uniformly distributed probability of the degree of deviation. The linearly decaying probability is more realistic for the geometrical parameters since, for example, the antenna will be more likely to be tilted by just one degree rather than five. For the ground parameter variations, we used a uniform probability for the deviations from the default values within the expected systematic uncertainties. We investigated the effects of the variations separately and, to obtain an overall systematic uncertainty, we investigated a mixture of all geometrical and ground conditions together.

2.2 Results and findings

We list the results of the reconstructed electromagnetic energy uncertainty caused by various systematic deviations in Tab. 3. We used two approaches to deal with a few outliers that drag the mean and standard deviation. First, we calculated the mean and standard deviation on 1 to 99 percentile values and, second, within the interval between ±15%. We consider the truncated mean and standard deviation the most objective ones, but to be complete, we also give all the other values.

Table 3: Statistical values for the uncertainties on the reconstructed electromagnetic energies caused by systemativ uncertainties of the antenna set-up. All values are in percents.

	all modified models	all modified geometries (48% default model)	all modified geometries (12% default model)	only modified ground	tilted antenna (linearly decaying probability)	tilted antenna (uniform probability)	rotated antenna (linearly decaying probability)	rotated antenna (uniform probability)	tilted station (linearly decaying probability)	tilted station (uniform probability)	shifted components (uniform probability)
Median	-0.47	-0.03	-0.11	-0.92	-0.16	-0.39	-0.07	-0.17	-0.08	-0.15	-0.03
Mean	-0.85	-0.02	-0.06	-1.63	-0.07	-0.20	-0.08	-0.07	0.02	-0.15	-0.02
Standard deviation	6.41	3.74	5.52	8.36	5.37	6.74	3.81	4.97	5.62	3.43	2.84
Truncated Mean (1st-99th percentile)	-0.96	-0.09	-0.15	-1.76	-0.17	-0.35	-0.14	-0.19	-0.10	-0.16	-0.04
Truncated Std.Dev. (1st-99th percentile)	3.18	1.09	1.46	4.36	1.83	2.50	1.37	1.85	1.27	1.68	0.29
Mean (within +/- 15%)	-0.85	-0.08	-0.15	-1.49	-0.16	-0.35	-0.13	-0.19	-0.10	-0.14	-0.05
Standard deviation (within +/- 15%)	3.23	1.50	1.86	4.13	2.21	2.81	1.77	2.25	1.70	2.04	0.88

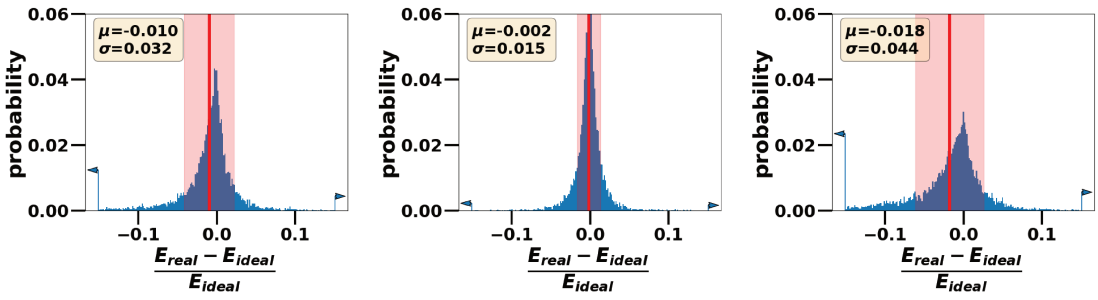

(a) (b) (c)

Figure 1: Histograms of deviations of the reconstructed electromagnetic energy for cases when (a) all modified models are used, (b) only models with modified geometry, (c) only modified models with changed ground parameters. Numbers on the x-axis are fractions.

We show the distributions of the deviations on the reconstructed electromagnetic energy for variations of the ground conditions, the geometry, and all combined in Fig. 1. The shape of the distribution resembles a Laplace distribution. From the figures, it is apparent that the systematic uncertainties of the ground parameters yield a more significant deviation ($\sim$ 4% uncertainty), making it a more important factor than the geometrical uncertainties ($<$ 2% uncertainty). Moreover, the uncertainties in the ground parameters introduce a non negligible bias. When using all of the modified antenna models, the uncertainty on the truncated samples is around 3%. Very conservatively, considering all statistics and various cases from Tab. 3, the systematic deviation caused by the antenna model systematic uncertainties should not be more than 5%.

To study the correlations of the electromagnetic energy deviations caused by the systematic uncertainties of the antenna model with zenith angle, azimuth angle, and energies, we first resample

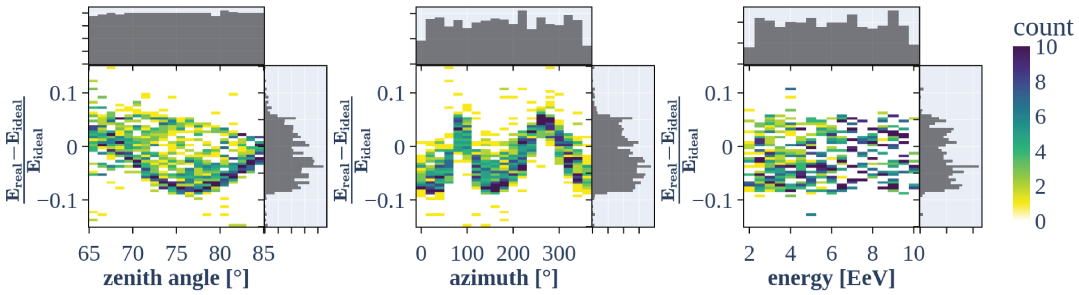

Figure 2: Example of the correlation between the deviation on the reconstructed electromagnetic energy and the (a) zenith angle, (b) azimuth angle and (c) energy using different ground conditions in the realistic scenario. In the this case ground number 6 from Tab. 2 was used.

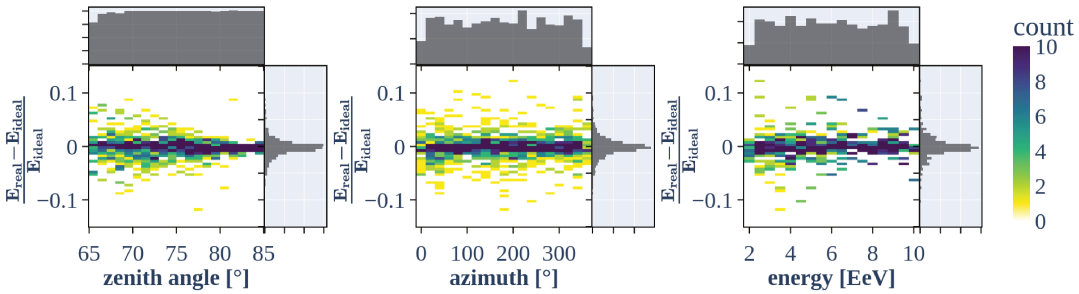

Figure 3: Example of the correlation between the deviation on the reconstructed electromagnetic energy and the (a) zenith angle, (b) azimuth angle and (c) energy using geometrically deviated antenna model (tilted antenna) in the realistic scenario.

them so that each bin contains approximately the same number of samples. Overall, the deviations do not correlate with the energy for any systematic variation. Deviations caused by the uncertainties in the ground conditions, as shown in Fig. 2, are strongly correlated with zenith angles and azimuth angles. The azimuthal dependency is likely to be caused mainly by the large SSD located just beneath the antenna, shielding the ground in the east-west direction, causing unequal azimuthal sensitivity to the ground conditions. With increasing zenith angle, the antenna pattern becomes more influenced by the ground conditions, hence the increasing correlation with increasing zenith angle. The sensitivity towards the horizon is suppressed by the bottom resistor, thus, the correlation drops.

There is no significant azimuthal dependency for the geometrical deviations as depicted in Fig. 3. Note that we did not use any preferred direction of the tilt or rotation; all are equally probable. We see that as the zenith angle increases, the deviations become significantly smaller. The reason behind this is the increasing number of stations that record a signal above threshold with increasing zenith angle and the probability of having a station with a certain degree of misalignment in the sample. An example of this effect is shown in Fig. 4. For low zenith angles, only a few stations record a signal above threshold; very rarely will there be a station without a systematic deviation. On the other hand, many stations with signals above threshold at high zenith angles will be without (large) systematic variations and only a few with the highest degree of deviations.

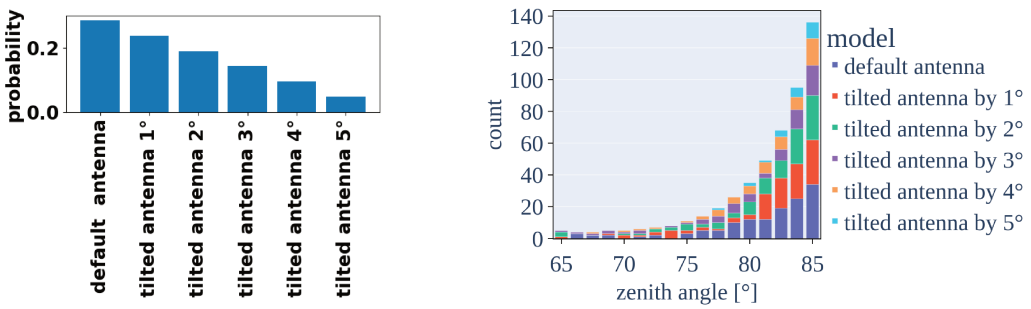

(a) **(b)**

Figure 4: Example of stations sampling with increasing zenith angle for the case of tilted antennas. (a) Probability of each model to be drawn when assigning antenna model to station. (b) Distribution of the drawn models on the full array as a function of zenith.

3. Effect of the geometrical systematic uncertainties on the antenna calibration

As next step we aim to investigate the effect of the previously discussed systematic uncertainties of the antenna set-up on the antenna calibration. We use the galactic radio emission to perform the absolute calibration of the radio antenna. However, besides the choice of radio sky map and fitting method, the calibration also depends on the antenna modeling, which then contributes to the systematic uncertainty of the absolute calibration.

3.1 Method and results

First, we simulated the galactic signal seen by a radio station, using a galactic map, an antenna model and a measured hardware response. We used five different sky temperature map models, and to evaluate the effect of the antenna model, we calculated the calibration parameters using 17 different antenna models. In particular: seven models with different ground conditions (Tab. 2), six with geometrically shifted components SSD and solar panel (horizontally shifted by 20, 10, 5 cm, horizontally shifted solar panel by 20 cm, vertically shifted SSD by 10 cm and horizontally and vertically shifted SSD by 10 cm) and four with omitted components (no WCD tank, no SSD, no SSD and solar panel, only radio antenna). Next, we fit the simulated galactic signal with four different fitting methods to derive the calibration parameters. This process is performed for channel 0 in the east-west (EW) antenna orientation and channel 1 in the north-south (NS) antenna orientation. In total, combinations of all of these factors gave 340 calibration parameters, which we then smeared by the underlying uncertainty of the map. Finally, we derived the final calibration parameters and their uncertainty from the smeared distribution. Both can be found in Tab. 4. For more details, see [6].

By fixing the sky temperature model and the fitting method, we investigated the effect of the antenna model on the calibration parameters. We found that the absolute calibration is robust against the choice of the antenna model (hence also against the systematic uncertainties of the actual setup) since the uncertainty caused by the antenna model is maximally 1.5%. The results are listed in Tab. 5.

Table 4: Calibration parameters. The first uncertainty is propagated from the simulated dataset. The second is the uncertainty propagated from the measured dataset.[6]

channel	voltage calibration parameter
EW	1.03±9.6%±2.0%
NS	0.96±9.7%±2.0%

Table 5: Effect of the different factors (in percents) on the calibration parameter. Modified from [6]

factor	min	max	mean
antenna model	0.3	1.4	0.9
antenna - different ground	0.2	1.8	1.0
antenna - shifted components	0.1	0.7	0.4
antenna - missing components	0.2	1.9	0.6

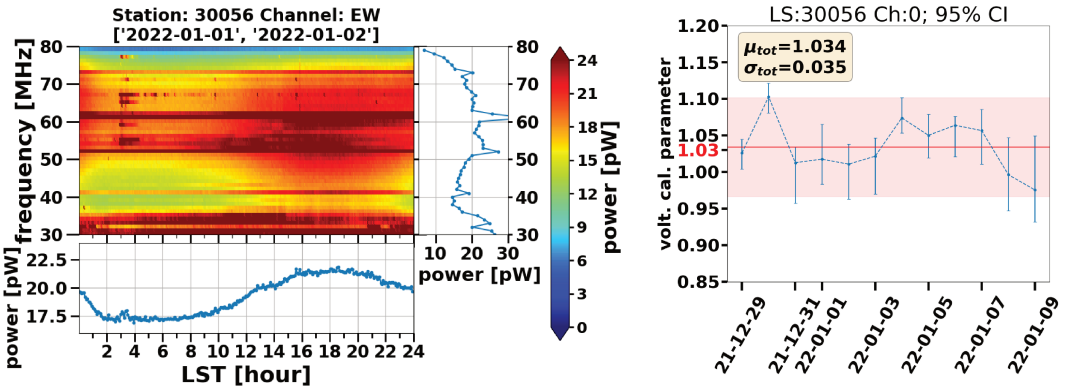

(a) (b)

Figure 5: (a) Noise as a function of the local sidereal time (LST) derived from one-day data from the FPGA spectra. (b) Calculated calibration parameters for station number 56 for each day of the campaign.

3.2 Outlook – Towards a daily absolute Galactic calibration

We implemented an algorithm in the FPGA (Field Programmable Gate Arrays) of the digitizer that continuously takes time traces and convert them to frequency spectra. Such spectra are then averaged and transferred every 5 minutes, yielding a high-quality background noise spectrum. The algorithm filters broad-band RFI using a threshold filter acting in the time domain. We tested the algorithm in an experimental campaign that lasted for 12 days. The noise background acquired in one day was of the campaign was of significantly better quality than a previous dataset, which was extracted from 4 months of triggered data (compare 5 and Fig. 2 (a) from [6]).

The acquired spectra allow us to compute the calibration parameters for each day individually. An example of the calibration parameter time evolution for a chosen station is shown in Fig. 5, where one can see that the parameters for each day are within two standard deviations of the overall average. Such a trend we also observed in other stations. The average of all daily calibration parameters can then be used as a final calibration parameter and also allows for checking station-to-station fluctuations (Fig. 6). Another application is that the daily calibration parameters might be an effective monitoring tool. For example, a calibration parameter for a particular station outside the confidence interval may indicate a faulty station. We plan to include the averaged spectra from the FPGAs in the standard monitoring package.

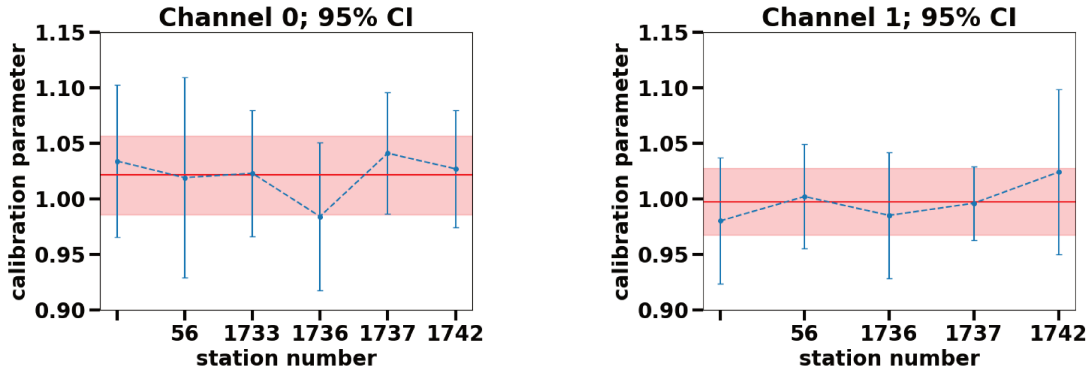

(a) **(b)**

Figure 6: Calibration parameters calculated using the averaged spectra from the FPGA for channel 0 (a) and channel 1 (b).

4. Conclusion

We studied the systematic effects introduced by the antenna model used in the analysis of the AugerPrime Radio Detector. We found the reconstructed electromagnetic energy robust against geometrical and ground parameter uncertainties in the antenna model. The ground appeared to be the most significant factor in the modeling ($\sim 4\%$ deviation). On the other hand, geometric antenna uncertainties are less relevant than ground parameter variations ($< 2\%$ deviation) and decrease with increasing zenith angle. Therefore, very conservatively, the uncertainty caused by the antenna modeling should not be larger than 5%. Further, we showed that the contribution from the antenna modeling on the absolute calibration is very small, maximally about 1.5%. Finally, we reported our efforts for online FPGA spectra averaging. The algorithm was successfully tested and yielded high-quality noise datasets that can be used as a calibration and monitoring tool.

Acknowledgement

This project is supported by the European Research Council advanced grant #787622 and the Dutch research Council.

References

[1] A. Castellina for the Pierre Auger Collaboration, *AugerPrime: the Pierre Auger Observatory Upgrade*, *EPJ Web of Conferences* **210** (2019) 06002.

[2] J.R. Hörandel for the Pierre Auger Collaboration, *A large radio array at the Pierre Auger Observatory: Precision measurements of the properties of cosmic rays at the highest energies*, *EPJ Web Conf.* **216** (2019) 01010.

[3] O. Krömer, H. Gemmeke, W. Apel, J.C. Arteaga, T. Asch, F. Badea et al., *New antenna for radio detection of uhecr*, *31st International Cosmic Ray Conference* (2009) 1232.

[4] https://www.qsl.net/4nec2/.

[5] A. Aab et al., *Calibration of the logarithmic-periodic dipole antenna (LPDA) radio stations at the Pierre Auger Observatory using an octocopter*, .

[6] T. Fodran for the Pierre Auger Collaboration, *First results from the AugerPrime Radio Detector*, *PoS* **ICRC2021** (2021) 270.